

Design and Characterization of HER-2-Targeted Gold Nanoparticles for Enhanced X-radiation Treatment of Locally Advanced Breast Cancer

Niladri Chattopadhyay,[†] Zhongli Cai,[†] Jean-Philippe Pignol,^{‡,§} Brian Keller,[‡]
Eli Lechtman,[‡] Reina Bendayan,[†] and Raymond M. Reilly^{*,†,||,⊥}

*Departments of Pharmaceutical Sciences, Medical Biophysics, and Medical Imaging,
University of Toronto, Department of Radiation Oncology, Sunnybrook Health Sciences
Centre, and Toronto General Research Institute, University Health Network,
Toronto, ON, Canada*

Received June 23, 2010; Revised Manuscript Received September 27, 2010; Accepted
October 25, 2010

Abstract: Our purpose was to develop a human epidermal growth factor receptor-2 (HER-2) targeted nanotechnology-based radiosensitizer. HER-2 is overexpressed in 20–30% of all breast cancers and up to 2-fold higher in locally advanced disease (LABC). Trastuzumab was derivatized with a polyethylene glycol (OPSS-PEG-SVA) cross-linker to produce trastuzumab-PEG-OPSS. These immunoconjugates were analyzed by SDS–PAGE, and their immunoreactivity was assessed by flow cytometry using HER-2 overexpressing SK-BR-3 breast cancer cells. Reacting trastuzumab with increasing ratios of PEG resulted in an increase in molecular weight from approximately 148 kDa to 243 kDa, associated with increasing PEG substitution (0.6 to 18.9 PEG chains per trastuzumab). Attachment of approximately 7 PEG chains per trastuzumab resulted in 56% retention in immunoreactivity assessed by flow cytometry. The conjugates were then linked to 30 nm AuNPs. Using a novel ¹²⁵Iodine-radiotracer based assay that overcomes the current limitations of spectrophotometric quantification of biological molecules on AuNPs we estimate 14.3 ± 2.7 antibodies were attached to each AuNP when 2×10^{11} AuNPs were reacted with 20 μ g of trastuzumab-PEG-OPSS. Specificity of trastuzumab-PEG-AuNPs for HER-2 and internalization in SK-BR-3 cells was demonstrated by comparing the uptake of trastuzumab-PEG-AuNPs or PEG-AuNPs by darkfield microscopy. The ability of trastuzumab-PEG-AuNPs in combination with 300 kVp X-rays to enhance DNA double strand breaks (DSBs) in SK-BR-3 cells was assessed by immunofluorescence using the γ -H2AX assay. γ -H2AX assay results revealed 5.1-fold higher DNA-DSBs with trastuzumab-PEG-AuNPs and X-radiation as compared to treatment with X-radiation alone. The trastuzumab-PEG-AuNPs are a promising targeted nanotechnology-based radiosensitizer for improving LABC therapy. The design and systematic approaches taken to surface modify and characterize trastuzumab-PEG-AuNPs described in this study would have application to other molecularly targeted AuNPs for cancer treatment.

Keywords: Gold nanoparticles (AuNPs); antibody per nanoparticle; trastuzumab (Herceptin); HER-2; PEGylation; X-radiation; radiosensitization; breast cancer; DNA damage

Introduction

Locally advanced breast cancer (LABC) carries a poor prognosis with only 1 out of every 2 patients surviving at 5

* Corresponding author. Mailing address: University of Toronto, Leslie Dan Faculty of Pharmacy, 144 College Street, Room 1204, Toronto, Ontario M5S 3M2, Canada. Tel: (416) 946-5522. Fax: (416) 978-8511. E-mail: raymond.reilly@utoronto.ca.

[†] Department of Pharmaceutical Sciences, University of Toronto.

[‡] Department of Medical Biophysics, University of Toronto.

[§] Department of Radiation Oncology, Sunnybrook Health Sciences Centre.

^{||} Department of Medical Imaging, University of Toronto.

[⊥] Toronto General Research Institute, University Health Network.

years due to metastasis to vital organs.¹ Furthermore, despite aggressive combinations of surgery, chemotherapy and radiation therapy, the locoregional recurrence rate of 10–20% remains high. There is a need for more efficient locoregional treatment without increasing the current toxicity of the radiosurgical combination. Some studies have shown a 2-fold higher incidence of the human epidermal growth factor receptor-2 (HER-2) expression in LABC compared to other forms of invasive BC with almost half of assessed patients having tumors that are HER-2-positive.^{2,3} This cell membrane receptor represents a unique opportunity to design novel targeted therapies including nanotechnology-based therapeutics.

Nanotechnology applications are being investigated in the field of radiation oncology. In recent years, use of high atomic (*Z*) number nanoparticles [e.g., gold nanoparticles (AuNPs)] to enhance the radiation absorbed dose deposited in tumors from X-radiation has been gaining increasing attention.^{4–7} It is well documented that X-rays interact with high-*Z* materials,^{8–12} and it is hypothesized that radiation

dose enhancement is a result of photoelectric absorption of X-rays⁹ with subsequent emission of Auger electrons.¹³ These electrons have a short range and deliver a precise and lethal dose in their immediate vicinity. This phenomenon is of great interest to radiation oncologists as the ability to target such materials preferentially to tumor cells could allow intracellular generation of these secondary electrons when the tumor cells are exposed to X-radiation. The therapeutic approach of using focused X-radiation only on the target tissue in conjunction with targeted AuNPs has a 2-fold advantage: (1) focused X-rays could spare normal tissue from the side effects of X-radiation, and (2) preferential dose enhancement in tumor cells loaded with targeted AuNPs could allow better tumor control per fraction of dose administered thereby improving the therapeutic outcome for the patient.

The purpose of our study was to develop clinically relevant targeted AuNPs. It is expected that these targeted AuNPs will selectively enhance DNA damage in malignant cells when used in conjunction with low energy X-rays. Using HER-2 as a clinically validated molecular target, and trastuzumab (Herceptin; Hoffman-La Roche) as a targeting agent, in this report, we describe the systematic development and characterization of HER-2 targeted AuNPs. Finally, we have also studied the ability of these targeted AuNPs to enhance DNA double-strand breaks when used in conjunction with 300 kVp X-rays.

Materials and Methods

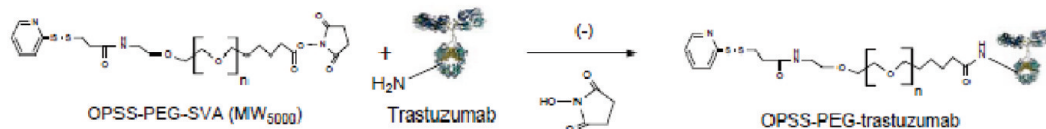
(A) PEGylation of Trastuzumab. PEGylation of trastuzumab was achieved through modification of ϵ -amino groups on the lysine residues. In this reaction PEG chains were attached to trastuzumab using a bifunctional cross-linker {Figure 1A [orthopyridyldisulfide-polyethyleneglycol-*N*-hydroxysuccinimide (OPSS-PEG-SVA, Laysan Bio, Arab, AL), molecular weight 5 kDa]}. Briefly, 100 μ L of trastuzumab (1 μ g/ μ L, PBS, pH 6.0) was reacted with a varying molar excess (1:1 to 250:1) of the OPSS-PEG-SVA (50 μ L, 100 mM NaHCO₃) overnight at 4 °C. The conjugates were then purified and buffer exchanged into PBS, pH 7.5, using ultrafiltration [(Vivaspin 30 kDa MW cutoff), Sartorius, Bohemia, NY].

(B) Characterization of PEGylated Trastuzumab. *SDS-PAGE and Size-Exclusion HPLC.* The purity and homogeneity of trastuzumab-PEG-OPSS immunoconjugates were evaluated by sodium dodecyl sulfate–polyacrylamide gel electrophoresis (SDS–PAGE) on a 5% Tris-HCl minigel (Bio-Rad, Mississauga, ON) electrophoresed under nonreducing conditions. Using SDS–PAGE, the attachment of

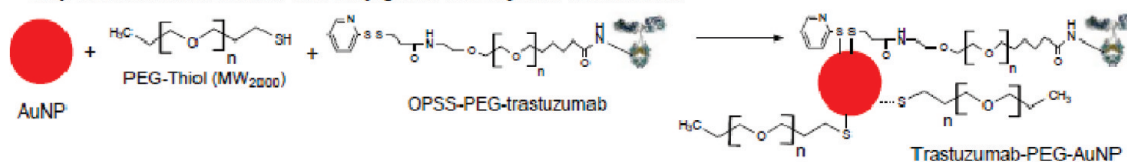
- (1) Fisher, B.; Anderson, S.; Bryant, J.; Margolese, R. G.; Deutsch, M.; Fisher, E. R.; Jeong, J.-H.; Wolmark, N. Twenty-year follow-up of a randomized trial comparing total mastectomy, lumpectomy, and lumpectomy plus irradiation for the treatment of invasive breast cancer. *N. Engl. J. Med.* **2002**, *347*, 1233–1241.
- (2) Sawaki, M.; Ito, Y.; Akiyama, F.; Tokudome, N.; Horii, R.; Mizunuma, N.; Takahashi, S.; Horikoshi, N.; Imai, T.; Nakao, A.; Kasumi, F.; Sakamoto, G.; Hatake, K. High prevalence of HER-2/neu and p53 overexpression in inflammatory breast cancer. *Breast Cancer* **2006**, *13*, 172–178.
- (3) Charafe-Jauffret, E.; Tarpin, C.; Bardou, V.-J.; Bertucci, F.; Ginestier, C.; Braud, A.-C.; Puig, B.; Geneix, J.; Hassoun, J.; Bimbaum, D.; Jacquemier, J.; Viens, P. Immunophenotypic analysis of inflammatory breast cancers: Identification of an 'inflammatory signature'. *J. Pathol.* **2004**, *202*, 265–273.
- (4) Herold, D. M.; Das, I. J.; Stobbe, C. C.; Iyer, R. V.; Chapman, J. D. Gold microspheres: A selective technique for producing biologically effective dose enhancement. *Int. J. Radiat. Biol.* **2000**, *76*, 1357–1364.
- (5) Hainfeld, J. F.; Slatkin, D. N.; Smilowitz, H. M. The use of gold nanoparticles to enhance radiotherapy in mice. *Phys. Med. Biol.* **2004**, *49*, N309–N315.
- (6) Kong, T.; Zeng, J.; Yang, J.; Yao, Y.; Wang, X.; Li, P.; Yang, A.; Roa, W.; Xing, J.; Chen, J. Surface modifications of gold nanoparticles to enhance radiation cytotoxicity. *2007 IEEE/NIH Life Science Systems and Applications Workshop, LISA*; 2008; pp 265–268.
- (7) Zheng, Y.; Hunting, D. J.; Ayotte, P.; Sanche, L. Radiosensitization of DNA by gold nanoparticles irradiated with high-energy electrons. *Radiat. Res.* **2008**, *169*, 19–27.
- (8) Howell, R. W. Auger processes in the 21st century. *Int. J. Radiat. Biol.* **2008**, *84*, 959–975.
- (9) Larson, D.; Bodell, W. J.; Ling, C.; Phillips, T. L.; Schell, M.; Shrieve, D.; Troxel, T. Auger electron contribution to bromodeoxyuridine cellular radiosensitization. *Int. J. Radiat. Oncol. Biol. Phys.* **1989**, *16*, 171–176.
- (10) Pignol, J.-P.; Rakovitch, E.; Beachey, D.; Le Sech, C. Clinical significance of atomic inner shell ionization (ISI) and Auger cascade for radiosensitization using IUDR, BUdR, platinum salts, or gadolinium porphyrin compounds. *Int. J. Radiat. Oncol. Biol. Phys.* **2003**, *55*, 1082–1091.

- (11) Spiers, W. *Br. J. Radiol.* **1949**, *22*, 512.
- (12) Takakura, T. Auger effects on bromo-deoxyuridine-monophosphate irradiated with monochromatic X-rays around bromine K-absorption edge. *Radiat. Environ. Biophys.* **1989**, *28*, 177–184.
- (13) Hainfeld, J. F.; Dilmanian, F. A.; Slatkin, D. N.; Smilowitz, H. M. Radiotherapy enhancement with gold nanoparticles. *J. Pharm. Pharmacol.* **2008**, *60*, 977–985.

A Step 1: PEGylation of Trastuzumab with OPSS-PEG-SVA



Step 2: Stabilisation of AuNP and conjugation to PEGylated Trastuzumab



Molecular Pharmaceutics

B

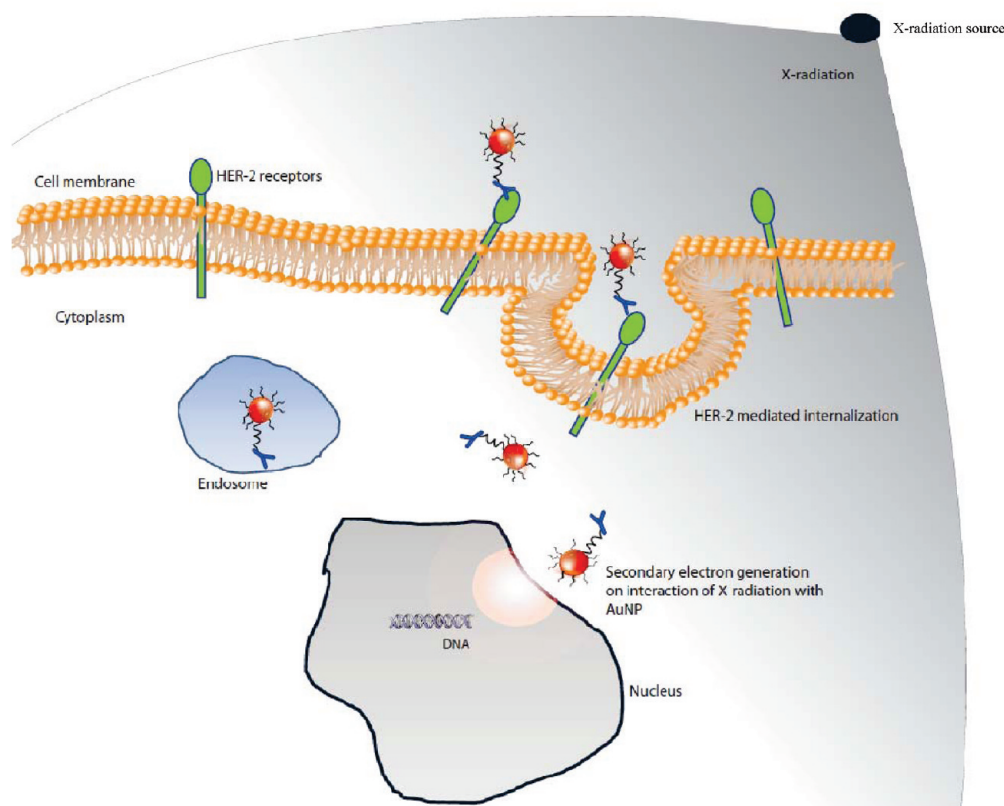


Figure 1. (A) Step-wise reactions for development of trastuzumab-PEG-AuNP via lysine modification using OPSS-PEG-SVA. The disulfide bond in the PEG cross-linker covalently attaches PEGylated trastuzumab to the AuNPs through a gold–thiol bond. (B) Illustration of HER-2-mediated cellular internalization of trastuzumab-PEG-AuNPs. Following, HER-2 receptor mediated internalization AuNPs could be trapped in endosomes or be deposited in the cytoplasm where they would interact with X-radiation to produce damaging secondary electrons. The fate of the HER-2 receptor associated with AuNPs is unknown, but following internalization it could undergo degradation or be recycled back to the cell surface.

OPSS-PEG-SVA to trastuzumab was also confirmed using a PEG specific iodine–barium chloride stain¹⁴ in addition to a Coomassie blue stain used to identify the proteins. To

determine the number of OPSS-PEG-SVA conjugated to trastuzumab, the difference between the apparent molecular weight (MW) values for trastuzumab-PEG-OPSS and trastuzumab was divided by the MW of OPSS-PEG-SVA (5189 Da) as determined by SDS–PAGE. Size-exclusion HPLC (SE-HPLC) on a Waters 600 system (Waters Corporation, Milford, MA) fitted with a BioSep-SEC-S2000 column

(14) Kurfurst, M. M. Detection and molecular weight determination of polyethylene glycol- modified hirudin by staining after sodium dodecyl sulfate-polyacrylamide gel electrophoresis. *Anal. Biochem.* **1992**, *200*, 244–248.

(Phenomenex, Torrance, CA) and a Waters 717 plus autosampler was used to assess the purity of the trastuzumab-PEG conjugates. Samples were eluted with 150 mM sodium chloride/10 mM sodium phosphate buffer, pH 7.5, at a flow rate of 1.0 mL/min. Peaks were detected using a Waters 2998 photodiode array detector set at 280 nm.

Immunoreactivity of PEGylated Trastuzumab. To evaluate the retention of HER-2 immunoreactivity of trastuzumab-PEG-OPSS conjugates prepared at different ratios of OPSS-PEG-SVA:trastuzumab (1:1 to 250:1) the binding to HER-2 overexpressing SK-BR-3 human breast cancer cells ($1-2 \times 10^6$ receptors/cell) was assessed by flow cytometry.¹⁵ SK-BR-3 cells were obtained from the American Type Culture Collection and cultured in RPMI 1640 media with 10% fetal bovine serum containing 100 U/mL of penicillin. Briefly, 1×10^6 cells were incubated for 1 h at 4 °C with trastuzumab or trastuzumab-PEG-OPSS conjugates followed by three rinses with PBS containing 0.1% sodium azide and 5% fetal bovine serum. The cells were then incubated at 4 °C for 1 h with a secondary antibody (fluorescein-isothiocyanate-labeled mouse anti-human IgG), rinsed again, and analyzed by a FACScalibur flow cytometer (BD Biosciences, San José, CA). Data were analyzed using Cellquest software (BD Biosciences). SK-BR-3 cells treated with the secondary antibody in the absence of trastuzumab pretreatment were used as a control.

A sample of trastuzumab-PEG conjugate obtained by reacting trastuzumab with a 25-fold molar excess of OPSS-PEG-SVA was selected based on its preserved immunoreactivity. Confocal microscopy was then used to directly compare the immunoreactivity and visualize the cellular distribution of trastuzumab and trastuzumab-PEG conjugates. Briefly, SK-BR-3 cells were plated on 8-well chamber slides (Nunc; Life Technologies, Rochester, NY) and cultured overnight at 37 °C/5% CO₂ in complete medium. After three gentle rinses with PBS, pH 7.5, the cells were incubated with trastuzumab or trastuzumab-PEG-OPSS conjugates and cultured for an additional 20 h in complete medium. The cells were then fixed with 3.7% para-formaldehyde and permeabilized for 10 min with Triton X-100 buffer (0.1% Triton X-100, 1% bovine serum albumin and 2% goat serum in PBS, pH 7.5). Nonspecific binding was blocked for 1 h with 10% goat serum (Sigma-Aldrich, St Louis, MO). After 3 further rinses, the slides were incubated with AlexaFluor 488 anti-human IgG (Molecular Probes, Carlsbad, CA). The slides were then mounted with Vectashield mounting media containing the nuclear stain 4,6-diamidino-2-phenylindole (DAPI) (Vector Laboratories, Burlington, ON) and sealed. Images were taken with a Zeiss LSM confocal microscope and processed with Adobe Photoshop Ver. 7.0 (San José, CA).

(C) Conjugation of PEGylated Trastuzumab to AuNPs.

Stabilization of AuNPs: Flocculation Assay. Prior to conjugating PEGylated trastuzumab to AuNPs, it was necessary to stabilize the AuNPs. AuNPs were stabilized using PEG-SH [MW 2 kDa, (Iris Biotech GmbH, Marktredwitz, Germany)]. It was expected that the shorter (MW = 2 kDa) PEG-SH chains would stabilize

the AuNPs. By conjugating trastuzumab to AuNPs via a longer (MW = 5 kDa) OPSS-PEG-SVA chain we designed the PEGylated trastuzumab to extend away from the 2K-PEG-SH stabilized AuNP surface thereby circumventing any potential steric hindrance to receptor binding that may arise due to the dense 2K-PEG-SH surface coating. Stability of PEG-AuNP to aggregation in a 1% NaCl solution was measured by absence of a dramatic red shift in the characteristic plasmon absorption peak (500 to 600 nm),¹⁶⁻¹⁸ and by Dynamic Light Scattering (DLS). In a typical assay, 1.0 mL of AuNPs [$(2 \times 10^{11}$ particles/mL), Ted Pella, Redding, CA] was incubated with varying molar excess of PEG-SH (1:1 to 15,000:1) for 1 h at room temperature. Following this step, the AuNPs were purified by centrifuging at 2500g for 30 min at 4 °C followed by centrifuging at 15000g for 30 min at 4 °C. Excess PEG-SH in supernatant was removed, and the AuNPs were resuspended in 900 μ L of double-deionized water (DDIW). Next, 100 μ L of 10% NaCl was added to each sample to trigger aggregation. The absorbance of samples at 524 nm (λ_{\max} of 30 nm AuNPs) was monitored using a UV-visible spectrophotometer, and results were expressed as a percentage of a control consisting of unmodified AuNPs (2×10^{11} particles). Particle size was measured by dynamic light scattering (DLS; Z-average) using a Malvern Zetasizer Nano-ZS (Malvern Instruments, Malvern, U.K.). Each DLS measurement was carried out in duplicate at a 90° angle at 25 °C. Each sample run consisted of 15 measurements.

Conjugation of PEGylated Trastuzumab to AuNPs and Monitoring of Changes in AuNP Hydrodynamic Radius. Following PEGylation of trastuzumab, the thiol-terminus of the PEG linker was used to covalently^{19,20} bind the immunoconjugates to AuNPs using the well-recognized strong gold-thiol interaction.²¹ The AuNPs were surface-coated simultaneously using the minimum amount of PEG-SH required for stabilization as determined by the flocculation assay. Briefly, trastuzumab-PEG-AuNPs were prepared by first adding 20 μ L of 250 μ M PEG-SH to the AuNPs and

- (15) McLarty, K.; Reilly, R. M. Molecular imaging as a tool for personalized and targeted anticancer therapy. *Clin. Pharmacol. Ther.* **2007**, *81*, 420-424.
- (16) Chithrani, B. D.; Ghazani, A. A.; Chan, W. C. W. Determining the size and shape dependence of gold nanoparticle uptake into mammalian cells. *Nano Lett.* **2006**, *6*, 662-668.
- (17) Liu, J.; Hu, W.; Chen, H.; Ni, Q.; Xu, H.; Yang, X. Isotretinoin-loaded solid lipid nanoparticles with skin targeting for topical delivery. *Int. J. Pharm.* **2007**, *328*, 191-195.
- (18) Liu, Y.; Shipton, M. K.; Ryan, J.; Kaufman, E. D.; Franzen, S.; Feldheim, D. L. Synthesis, stability, and cellular internalization of gold nanoparticles containing mixed peptide-poly(ethylene glycol) monolayers. *Anal. Chem.* **2007**, *79*, 2221-2229.
- (19) Zhang, D.; Neumann, O.; Wang, H.; Yuwono, V. M.; Barhoumi, A.; Perham, M.; Hartgerink, J. D.; Wittung-Stafshede, P.; Halas, N. J. Gold nanoparticles can induce the formation of protein-based aggregates at physiological pH. *Nano Lett.* **2009**, *9*, 666-671.
- (20) Shenoy, D.; Fu, W.; Li, J.; Crasto, C.; Jones, G.; DiMarzio, C.; Sridhar, S.; Amiji, M. Surface functionalization of gold nanoparticles using hetero-bifunctional poly(ethylene glycol) spacer for intracellular tracking and delivery. *Int. J. Nanomed.* **2006**, *1*, 51-57.

then immediately adding 20 μg , 10 μg or 5 μg of trastuzumab-PEG-OPSS in PBS, pH 7.5. This method of rapid sequential addition allowed the trastuzumab-PEG-OPSS to compete with the shorter PEG-SH used for AuNP stabilization for conjugation to the available nanoparticle surface area. The reaction was carried out in low binding microfuge tubes (Axygen Scientific Inc., Union City, CA) and allowed to proceed for 1 h at 4 °C. The AuNPs were purified by centrifuging at 2500g for 30 min at 4 °C followed by centrifuging at 15000g for 30 min at 4 °C. This two-step centrifugation process minimized adhesion of AuNPs to the tube walls. One mL of the supernatant was removed, and the pellet was resuspended by adding 1 mL of PBS, pH 7.5. Changes in particle size were assessed at each step of the AuNP bioconjugation procedure by DLS using the procedure outlined for the flocculation assay.

Quantification of the Number of Trastuzumab-PEG-OPSS per AuNP. The average number of trastuzumab-PEG molecules attached to each AuNP was determined by incorporating ^{125}I -labeled trastuzumab-PEG-OPSS into the AuNP conjugation reaction. Trastuzumab (2.0 mg, 10 mg/mL) was radioiodinated by incubation with 32–37 MBq of ^{125}I (MDS Nordion Inc., Kanata, ON) for 10 min using the Iodogen (1,3,4,6-tetrachloro-3 α ,6 α -diphenylglycouril; Sigma-Aldrich, St. Louis, MO) method before reacting with 25-fold molar excess of OPSS-PEG-SVA. ^{125}I -Trastuzumab was separated from unbound ^{125}I by ultrafiltration (50 kDa cutoff, Millipore, Billerica, MA). After purification, the radiochemical purity of ^{125}I -trastuzumab was routinely >96%. Radioactivity measurements were made using an automatic γ -counter (Wallace Wizard 1480; Perkin-Elmer, Waltham, MA). PEGylated ^{125}I -trastuzumab was then separated from unbound OPSS-PEG-SVA by ultrafiltration and conjugated to AuNPs as described earlier. After reacting 2×10^{11} AuNPs with ^{125}I -labeled trastuzumab-PEG-OPSS, the AuNPs were purified by centrifugation. The supernatant (1 mL) containing excess ^{125}I -trastuzumab-PEG-OPSS was removed. The pellet was resuspended in 1 mL of PBS, pH 7.5, and transferred to a new low-binding microfuge tube to control for any radioactivity adsorbed onto the original reaction tubes. The coupling efficiency of ^{125}I -trastuzumab-PEG to AuNPs was determined by measuring the proportion of radioactivity bound to AuNPs. The number of AuNPs was calculated by measuring the absorbance at 524 nm and using the extinction coefficient ($3.585 \times 10^9 \text{ M}^{-1} \text{ cm}^{-1}$) for 30 nm AuNPs (BBInternational Lifesciences, U.K.). The number of ^{125}I -trastuzumab-PEG attached to each AuNP was calculated by dividing the moles of ^{125}I -trastuzumab-PEG by the moles of AuNP.

Verification of Trastuzumab Conjugation AuNPs Using Immunogold Transmission Electron Microscopy (TEM). Trastuzumab-PEG-AuNP or PEG-AuNP conjugates were incubated with 5 nm gold-labeled mouse anti-human IgG (Sigma-

Aldrich) for 1 h. Following this the AuNPs were centrifuged to separate 30 nm AuNPs from the secondary anti-human IgG-5 nm AuNP. Centrifuging at 15000g can separate 30 nm AuNPs from 5 nm AuNPs as the sedimentation rate for 5 nm AuNPs is significantly slower than that of 30 nm AuNPs. Samples were mounted on copper grids and imaged with a JEOL 2010 transmission electron microscope (JEOL Ltd., Tokyo, Japan).

(D) HER-2 Targeting: Evaluation of Internalization by Darkfield Microscopy. The HER-2-mediated internalization (Figure 1B) of trastuzumab-modified AuNPs was studied in SK-BR-3 cells by dark field microscopy TEM. Briefly, cells were cultured (6×10^4 cells/well) on 8-chamber slides (Nunc, Waltham, MA) overnight at 37 °C/5% CO_2 in growth medium. Confluent cells were then treated overnight with 0.8 mL of growth medium containing PBS, pH 7.5, trastuzumab-PEG-AuNPs or PEG-AuNPs. The concentration of AuNPs was adjusted to approximately 2×10^{11} particles/mL ($\sim 0.3 \text{ nM}$ of AuNPs). In some experiments, blocking of HER-2 was achieved by treating cells with 300 nM of trastuzumab for 2 h prior to incubating with AuNPs. Cells were then fixed with 4% paraformaldehyde for 15 min and subsequently incubated with 5.0 mg/mL wheat germ agglutinin-Alexa Fluor 594 (Molecular Probes, Inc., Carlsbad, CA) for 15 min to visualize the cell membrane. After two 5 min rinses with PBS, pH 7.5, the slides were mounted with Vectashield mounting media containing DAPI and kept at 4 °C overnight. Images were taken with an Olympus BX50 Upright microscope (Olympus Corp, Tokyo, Japan) in darkfield mode using a $20\times/0.55$ lens. Excitation was at 364 or 543 nm for visualization of DAPI or AlexaFluor-594, using 385–470 nm or 505–560 nm emission filters, respectively. Images were merged using ImagePro and stored as tiff files.

Clonogenic Assay. The toxicity of trastuzumab-PEG-AuNPs or PEG-AuNP to SK-BR-3 cells was assessed by a clonogenic assay. Subconfluent SK-BR-3 cells were incubated with trastuzumab-PEG-AuNP (2×10^{11} particles/mL) suspended in growth medium, PEG-AuNP (2×10^{11} particles/mL) suspended in medium or cells cultured in medium alone for 24 h. Cells were then washed three times with PBS, trypsinized and resuspended in fresh medium. Approximately 10^3 cells were seeded in triplicate into 6-well tissue culture plates containing medium. After being cultured at 37 °C and 5% CO_2 for 12 days, the cells were washed once with PBS and then stained with methylene blue (1% in a 1:1 mixture of ethanol and water). The number of colonies in each well was counted manually by light microscopy. The plating efficiency (PE) was determined by dividing the number of colonies formed in the untreated control dishes by the number of cells seeded. The surviving fraction (SF) was calculated by dividing the number of colonies formed by the number of cells seeded and then multiplying by the PE.

Evaluation of Trastuzumab-AuNP Enhanced and X-Radiation Induced DNA Double-Strand Breaks. The ability of trastuzumab-PEG-AuNPs and PEG-AuNPs to enhance DNA

(21) Qian, X.; Peng, X. H.; Ansari, D. O.; Yin-Goen, Q.; Chen, G. Z.; Shin, D. M.; Yang, L.; Young, A. N.; Wang, M. D.; Nie, S. In vivo tumor targeting and spectroscopic detection with surface-enhanced Raman nanoparticle tags. *Nat. Biotechnol.* **2008**, *26*, 83–90.

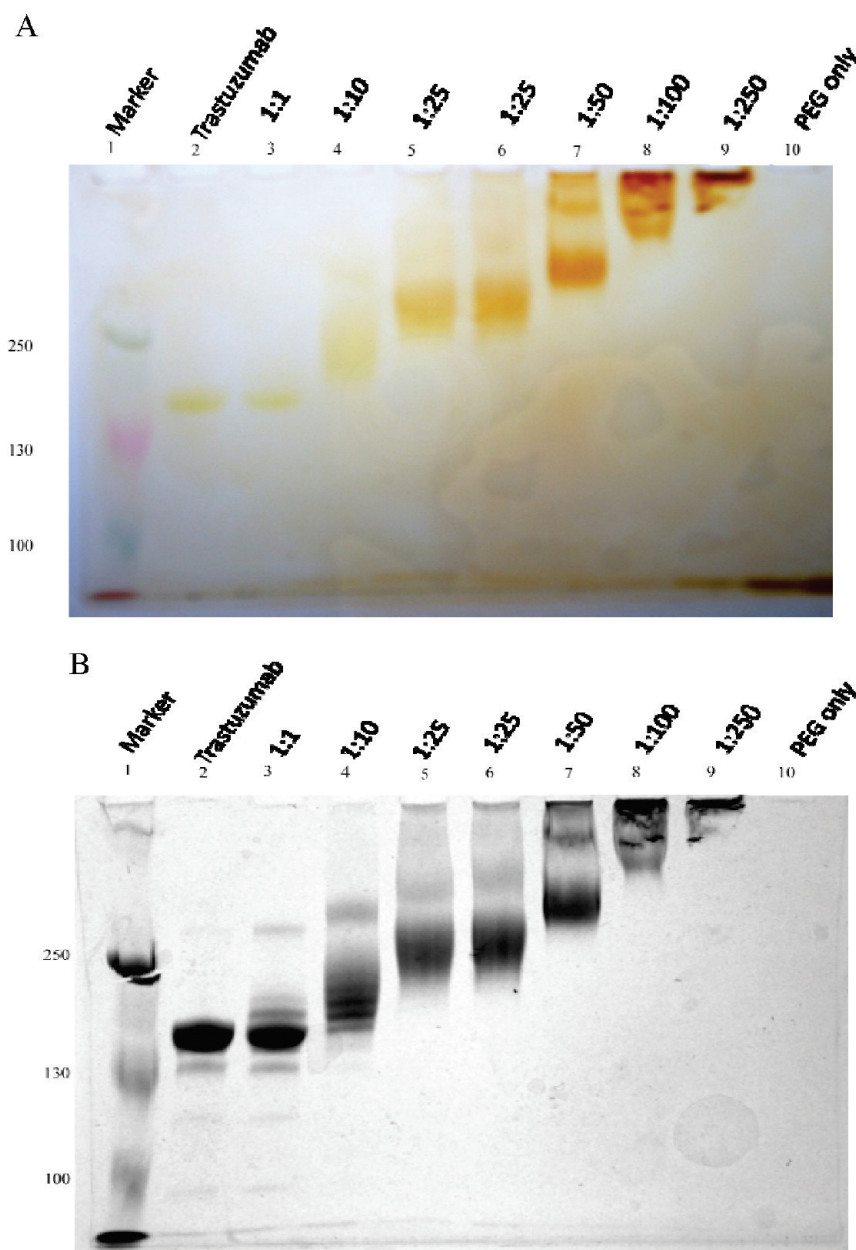


Figure 2. (A) SDS–PAGE with an iodine–barium chloride stain for PEG, and (B) with a Coomassie blue stain of trastuzumab (Tmab) (lane 2) or trastuzumab reacted with a 1-, 10-, 25-, 25-, 50-, 100-, or 250-fold molar excess of OPSS-PEG (lanes 3–9). Lane 10 was loaded with OPSS-PEG only. Lane 1 contains standard molecular weight markers (Kaleidoscope Prestained Marker, Bio-Rad) with the approximate molecular weights shown on the left of the gel. An increase in the apparent molecular weight of trastuzumab is observed when reacted with an increasing molar excess of OPSS-PEG-SVA. At lower OPSS-PEG-SVA:trastuzumab reaction ratios, a laddering effect is observed with the Coomassie blue stain suggesting incomplete reaction products.

double-strand breaks (DSBs) in SK-BR-3 cells exposed to 300 kVp X-rays was evaluated using the γ -H2AX assay. This assay detects the phosphorylation of histone-H2AX at serine-139 (γ -H2AX), which is visualized as discrete nuclear foci by immunofluorescence confocal microscopy using γ -H2AX-specific antibodies.²² Briefly, cells were cultured (6×10^4 cells/well) on 8-chamber slides overnight at 37 °C

in medium. Confluent cells were then treated overnight with 0.8 mL of growth medium containing PBS, pH 7.5, trastuzumab-PEG-AuNPs or PEG-AuNPs. The concentration of AuNPs was adjusted to 2×10^{11} particles/mL (~ 0.3 nM of AuNPs). The treated cells were then exposed to 0 to 1.0 Gy of X-radiation using an X-ray source (Gulmay orthovoltage X-ray system, model D3300; Surrey, U.K.), operating at 300 kVp. At this energy, the average photon energy is 140 keV. Cells were subsequently fixed 30 min postradiation and stained for γ -H2AX as previously reported.²³ Images were

(22) Peng, M.; Litman, R.; Jin, Z.; Fong, G.; Cantor, S. B. BACH1 is a DNA repair protein supporting BRCA1 damage response. *Oncogene* **2006**, 25, 2245–2253.

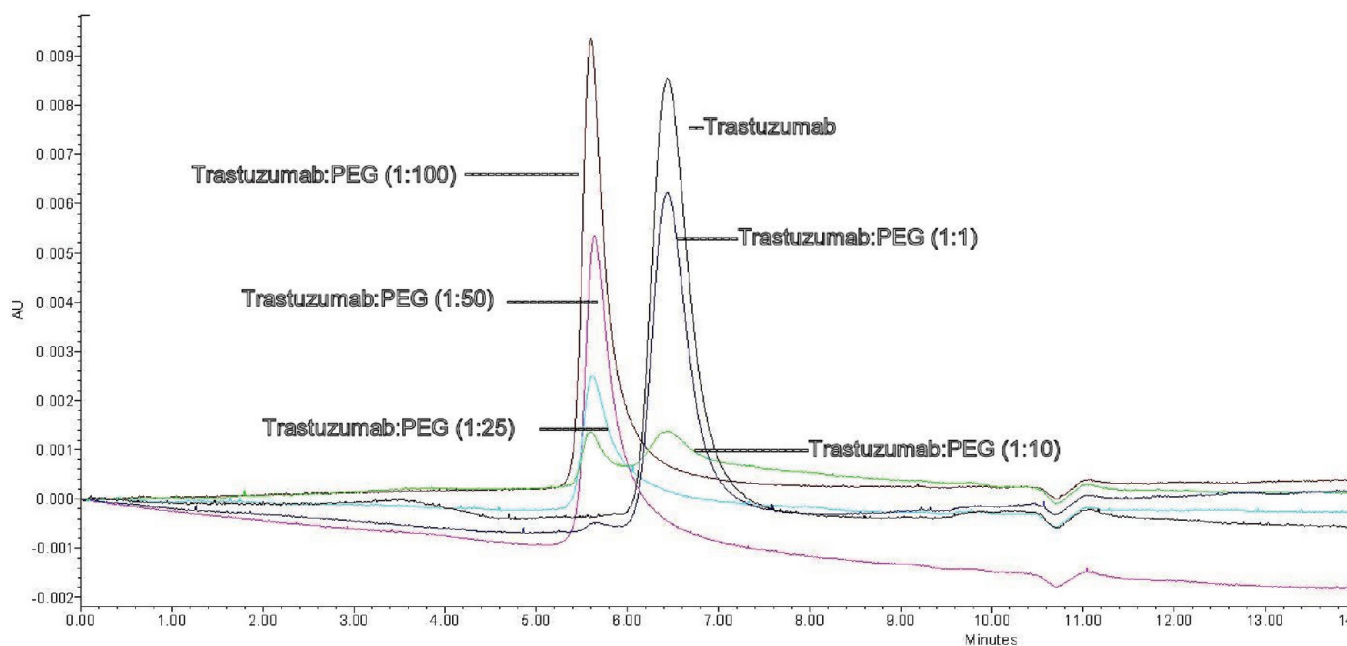


Figure 3. Size-exclusion HPLC chromatogram of trastuzumab-PEG conjugates analyzed on a BioSep-SEC-S2000 column eluted with 150 mM sodium chloride/10 mM sodium phosphate buffer, pH 7.5 at a flow rate of 1 mL/min, with detection using a UV detector set at 280 nm. Trastuzumab was eluted with a retention time (t_R) of 6.4 min. This t_R for trastuzumab:PEG (1:25, 1:50 and 1:100) was 5.6 min. The PEGylation reaction was incomplete for trastuzumab:PEG (1:1 and 1:10) with multiple peaks observed at 5.6 and 6.4 min. These data correlate well with the multiple bands seen on SDS-PAGE for the lower PEG reaction ratios.

taken with an inverted LSM510 confocal microscope (Carl Zeiss). Excitation was at 364 or 488 nm for visualization of DAPI or AlexaFluor-488 with emission filters of 385–470 nm or 505–550 nm, respectively. For visualization of γ -H2AX foci, 10–15 Z-stack images at 1.2 μ m intervals were acquired throughout the entire cell nucleus and merged using LSM-Viewer software (Version 3.5.0.376; Zeiss). The number of γ -H2AX foci present in each cell were quantified with ImageJ software (version 1.36b; National Institutes of Health) using customized macros developed recently by our group.²³

Statistical Analysis. Statistical comparisons among treatment groups were made using one way ANOVA using Prism, Ver. 4.03 (GraphPad Software Inc., San Diego, CA). Differences were considered significant at $p \leq 0.05$.

Results

Characterization of PEGylated Trastuzumab. PEGylation of trastuzumab was achieved by modification of amine groups on lysine residues on the IgG with OPSS-PEG-SVA (MW = 5 kDa). SDS-PAGE combined with dual staining for PEG (iodine–barium chloride stain; Figure 2A) and protein (Coomassie blue; Figure 2B) confirmed conjugation of OPSS-PEG-SVA to trastuzumab. Increasing the OPSS-PEG-SVA:trastuzumab ratio resulted in a gradual increase in the apparent MW of trastuzumab from approximately 148 kDa to 243 kDa, indicating increasing PEG substitution. According to the apparent estimated MW values from calibration of the gel, approximately 0.6, 1.2, 6.9, and 18.3 PEG chains were conjugated to trastuzumab at an OPSS-

PEG-SVA:trastuzumab molar ratio of 1:1, 10:1, 25:1 and 50:1, respectively. The higher molar ratios of 100:1 and 250:1 yielded conjugates that were much larger in size and did not migrate through the gel matrix. Size exclusion HPLC analysis of trastuzumab-PEG conjugates showed multiple peaks with retention times (t_R) at 5.6 and 6.4 min when trastuzumab was reacted with PEG at ratios of 1:1 and 10:1 and a single peak at reaction ratios higher than 25:1 (Figure 3).

Immunoreactivity of PEGylated Trastuzumab. Flow cytometry analysis (Figure 4A) of trastuzumab-PEG-OPSS conjugates demonstrated reduced binding when the OPSS-PEG-SVA:trastuzumab molar ratio was increased. When trastuzumab-PEG-OPSS conjugates were formed by reacting trastuzumab with a 25-fold molar excess of OPSS-PEG-SVA, the mean fluorescence intensity was approximately 56% of that for unmodified trastuzumab. A greater loss in HER-2 binding efficiency was observed at molar ratios of 50:1 and higher with only 25–30% immunoreactivity relative to trastuzumab observed. Confocal immunofluorescence microscopy confirmed the immunoreactivity of trastuzumab-PEG-OPSS immunoconjugates prepared at a molar ratio of 25:1 (Figure 4C). Due to the relatively preserved immunoreactivity of these immunoconjugates and the absence of residual unconjugated trastuzumab, they were used for all further experiments.

(23) Cai, Z.; Vallis, K. A.; Reilly, R. M. Computational analysis of the number, area and density of γ -H2AX foci in breast cancer cells exposed to ¹¹¹In-DTPA-hEGF or γ -rays using ImageJ software. *Int. J. Radiat. Biol.* **2009**, *85*, 262–271.

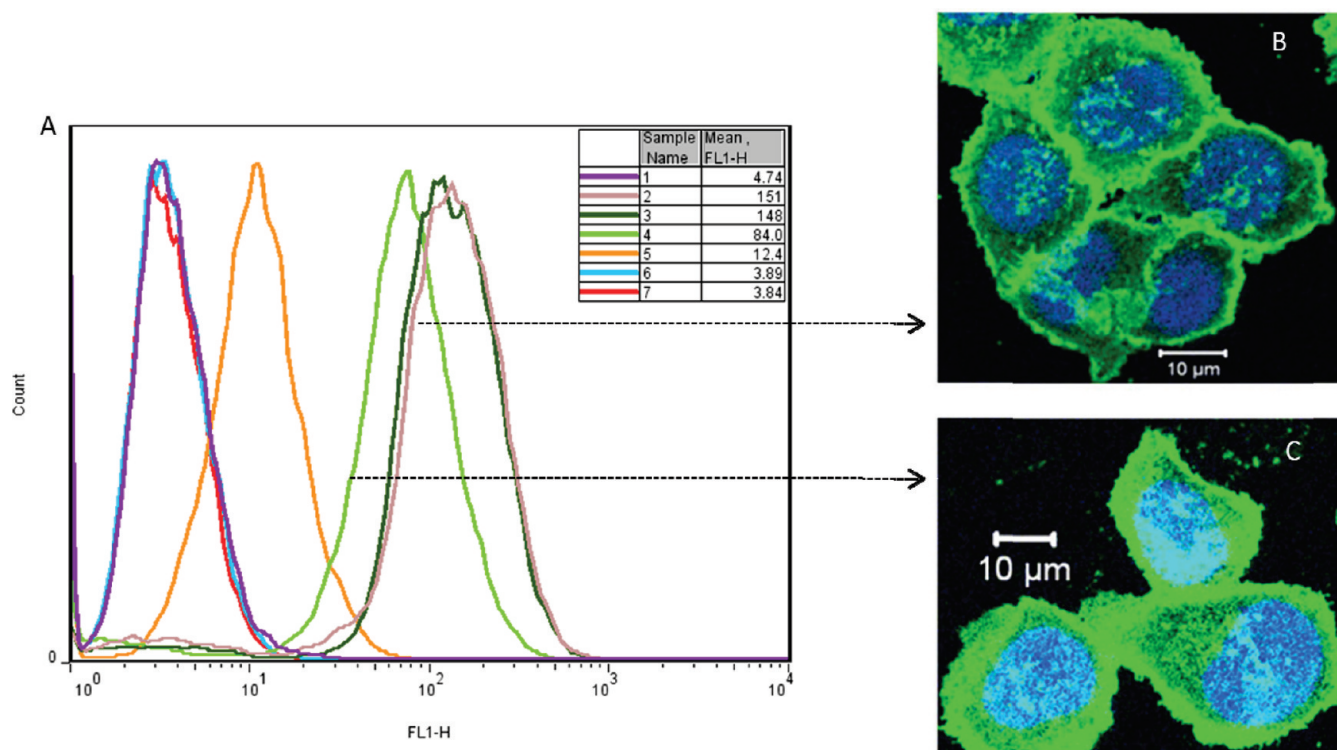


Figure 4. (A) Flow cytometry histogram plot showing fluorescence of trastuzumab-PEG conjugates associated with SK-BR-3 HER-2-overexpressing cells. Cells were treated with trastuzumab or trastuzumab-PEG-OPSS prepared by reacting increasing molar ratios OPSS-PEG-SVA:trastuzumab of (3) 10:1, (4) 25:1, (5) 50:1, (6) 100:1, and (7) 250:1. Mean fluorescence intensity (FL-1 H) is shown in the inset table. There is a decrease in immunoreactivity when the IgG:PEG reaction ratio is increased. Samples 1 and 2 represent cells treated with anti-human IgG labeled with FITC in the absence and presence of pretreatment with trastuzumab, respectively. In a separate experiment, confocal microscopy images of (B) SK-BR-3 cells treated with trastuzumab and (C) SK-BR-3 cells treated with trastuzumab-PEG-OPSS (prepared by reacting trastuzumab with a 25-fold molar excess of OPSS-PEG-SVA), respectively. These results confirm that PEGylated trastuzumab retains immunoreactivity toward HER-2 with internalization capability.

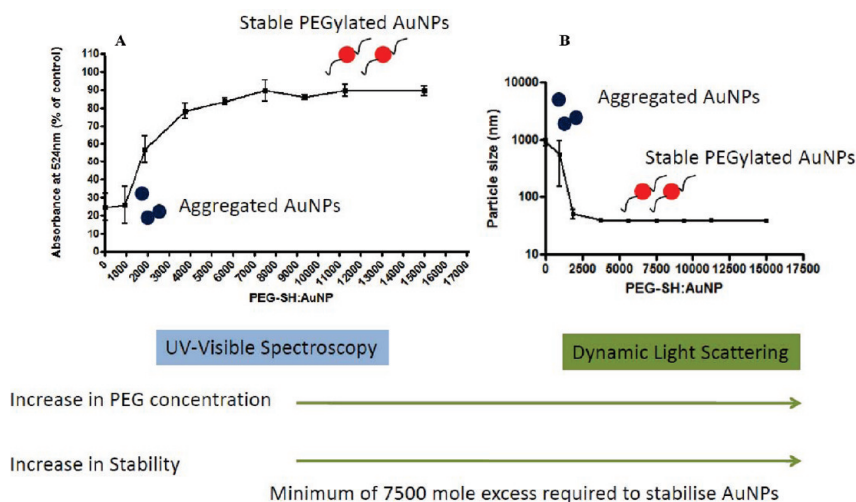


Figure 5. Stabilization of AuNPs with increasing concentration of mPEG-SH. Stability (lack of aggregation) in 1% NaCl was monitored by a decrease in absorbance (UV-visible spectroscopy, panel A) at 524 nm and a decrease in particle size (dynamic light scattering, panel B). These images illustrate that a minimum amount of PEG-SH is necessary to stabilize the AuNPs. Data represent the mean \pm SD result from three independent experiments.

Conjugation of PEGylated and Immunoreactive Trastuzumab to AuNPs. UV-visible spectroscopy and dynamic light scattering (Figure 5A,B) indicated that AuNPs were stabilized by reaction with a minimum 7,500-fold molar

excess of PEG-SH (MW = 2 kDa). Increasing the PEG-SH reaction ratio beyond this point did not further increase stability. Incomplete coating of the AuNP surface with PEG-SH resulted in unstable particles which aggregated in 1%

Table 1. Number of ^{125}I -Labeled Trastuzumab-PEG-OPSS Molecules Conjugated Per AuNP^a

trastuzumab-PEG-OPSS reacted with 2×10^{11} AuNPs, μg	no. of trastuzumab/ particle
20	18.4 ± 2.8
10	14.3 ± 2.7
5	10.2 ± 1.9

^a This table depicts the mean number \pm SD of ^{125}I -labeled trastuzumab-PEG-OPSS molecules conjugated per AuNP. Data represent the mean \pm SD result from three independent experiments.

NaCl to form micrometer-sized particles. In order to determine the average number of trastuzumab molecules attached to each AuNP, ^{125}I -labeled trastuzumab-PEG-OPSS immunoconjugates were incorporated into the reaction with AuNPs. Using this method, it was established (Table 1) that 18.5 ± 2.8 , 14.3 ± 2.7 and 10.2 ± 1.9 trastuzumab molecules were conjugated per AuNP when 2×10^{11} AuNPs were reacted with 20 μg , 10 μg and 5 μg of trastuzumab-PEG-OPSS, respectively. In the TEM image of the AuNP conjugates (Figure 6), binding of 5 nm gold-labeled secondary anti-human IgG antibodies to trastuzumab localized on the AuNP surface was observed. Using image analysis software, the measured distance from the surface of the AuNPs to the antibodies conjugated via the PEG cross-linker was 10–15 nm (Figure 6B). Coating with PEG was also visualized as a faintly dense corona surrounding the AuNPs (Figure 6A). The hydrodynamic size of the particles as assessed by DLS (Table 2) increased at each step of the reaction. For example, when reacting 2×10^{11} particles with 10 μg of PEGylated trastuzumab, the sizes were as follows: AuNPs (35.6 ± 1.9 nm), AuNP-PEG (42.1 ± 1.0 nm), and trastuzumab-PEG-AuNPs (54.2 ± 1.9 nm). Therefore, there was a hydrodynamic increase in size of 6.5 nm upon the addition of PEG-SH and an increase of 18.6 nm when trastuzumab-PEG was conjugated to the AuNPs. Short-term stability studies in 1% NaCl (Table 2) demonstrated that the particles remained stable in PBS, pH 7.5, with no increase in size when stored at 4 °C for 14 days.

HER-2 Targeting: Evaluation of Internalization by Dark-field Microscopy. Darkfield microscopy demonstrated uptake of trastuzumab-conjugated AuNPs by SK-BR-3 cells (Figure 7A). This uptake was inhibited when HER-2 were blocked by pretreating the cells with an excess (300 nM) of trastuzumab (Figure 7B). No signal due to light scattering from AuNPs was detected from SK-BR-3 cells incubated with control PEG-AuNPs (Figure 7C) demonstrating the ability of trastuzumab to efficiently transport conjugated AuNPs into HER-2 overexpressing cells.

Evaluation of Trastuzumab-PEG-AuNP Enhanced and X-radiation Induced DNA Double Strand Breaks. The induction of DNA double-strand breaks as measured by integrating the density of γ -H2AX foci in SK-BR-3 cells increased with the X-ray absorbed dose for all three treatment conditions (PBS, PEG-AuNPs or trastuzumab-PEG-AuNPs). The induction of DSB (Figure 8) for SK-BR-3 cells treated with trastuzumab-PEG-AuNPs and exposed to X-radiation

was enhanced 5.1-fold and 3.3-fold compared to that in cells treated with a combination of PEG-AuNPs or PBS and X-radiation ($p > 0.05$). There was no significant toxicity toward SK-BR-3 cells as assessed by clonogenic assay after treatment with either trastuzumab-PEG-AuNPs (mean surviving fraction, 1.00 ± 0.22) or PEG-AuNPs (surviving fraction, 0.93 ± 0.32) for 24 h ($p > 0.05$) when compared to cells cultured with medium only (mean surviving fraction, 1.00 ± 0.35) in the absence of X-radiation.

Discussion

AuNPs of 30 nm diameter were modified with trastuzumab-PEG-OPSS chains to bind them specifically to HER-2-positive SK-BR-3 breast cancer cells and mediate their internalization, and with shorter PEG chains to stabilize them to aggregation in solution. This HER-2 mediated internalization allowed enhancement of X-radiation induced DNA double-strand breaks likely through generation of subcellular range Auger electrons and longer range photoelectrons caused by the interaction of X-radiation with AuNPs. Modification of ϵ -amino groups on the lysine residues of trastuzumab using OPSS-PEG-SVA provided an efficient means of obtaining trastuzumab-PEG immunoconjugates with varying degree of PEG substitution, depending on the reaction conditions employed. This PEG cross-linker has a succinimidyl valerate group on one end for modification of amines on proteins and a disulfide bridge at the opposing terminus for direct conjugation to the AuNPs. Previous studies have demonstrated the sensitivity of antibodies to PEGylation with a 70–90% loss of antigen binding affinity frequently reported.^{24–29} Flow cytometry analysis of trastuzumab-PEG immunoconjugates indicated decreased immunoreactivity when the OPSS-PEG-SVA:trastuzumab reaction

- (24) Casey, J. L.; Pedley, R. B.; King, D. J.; Boden, R.; Chapman, A. P.; Yarranton, G. T.; Begent, R. H. J. Improved tumour targeting of di-Fab' fragments modified with polyethylene glycol. *Tumor Targeting* **1999**, *4*, 235–244.
- (25) Chapman, A. P. PEGylated antibodies and antibody fragments for improved therapy: A review. *Adv. Drug Delivery Rev.* **2002**, *54*, 531–545.
- (26) Kitamura, K.; Takahashi, T.; Yamaguchi, T.; Noguchi, A.; Noguchi, A.; Takashina, K.-i.; Tsurumi, H.; Inagake, M.; Toyokuni, T.; Hakomori, S.-i. Chemical engineering of the monoclonal antibody A7 by polyethylene glycol for targeting cancer chemotherapy. *Cancer Res.* **1991**, *51*, 4310–4315.
- (27) Kitamura, K.; Takahashi, T.; Takashina, K.; Yamaguchi, T.; Noguchi, A.; Tsurumi, H.; Toyokuni, T.; Hakomori, S. Polyethylene glycol modification of the monoclonal antibody A7 enhances its tumor localization. *Biochem. Biophys. Res. Commun.* **1990**, *171*, 1387–1394.
- (28) Pedley, R. B.; Boden, J. A.; Boden, R.; Begent, R. H. J.; Turner, A.; Haines, A. M. R.; King, D. J. The potential for enhanced tumour localisation by poly(ethylene glycol) modification of anti-CEA antibody. *Br. J. Cancer* **1994**, *70*, 1126–1130.
- (29) Suzuki, T.; Wu, D.; Schlachetzki, F.; Jian, Y. L.; Boado, R. J.; Pardridge, W. M. Imaging endogenous gene expression in brain cancer in vivo with ^{111}In -peptide nucleic acid antisense radiopharmaceuticals and brain drug-targeting technology. *J. Nucl. Med.* **2004**, *45*, 1766–1775.

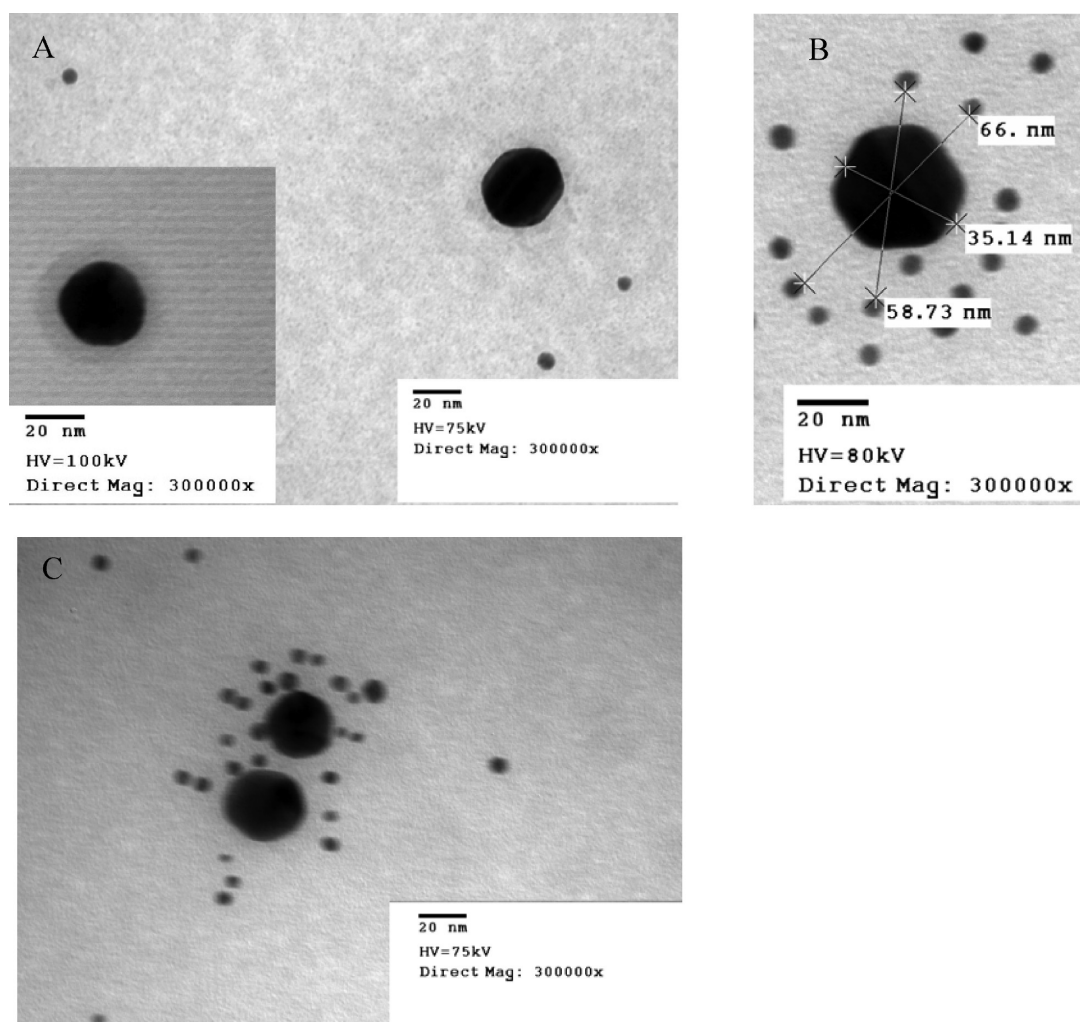


Figure 6. Transmission electron microscopy images of 5 nm gold labeled mouse anti-human IgG reacted with (A) PEG-AuNP, (B, C) trastuzumab-PEG-AuNP.

Table 2. Dynamic Light Scattering (DLS) Analysis of AuNPs Modified with Varying Concentrations of Trastuzumab-PEG-OPSS^a

	day 1	day 7	day 14
AuNP	35.6 ± 1.8	35.6 ± 1.5	37.0 ± 1.7
AuNP-PEG	42.1 ± 1.0	46.3 ± 4.1	45.4 ± 3.4
AuNP + PEG-trastuzumab (20 µg)	58.3 ± 1.5	56.1 ± 2.9	55.5 ± 1.3
AuNP + PEG-trastuzumab (10 µg)	54.2 ± 1.9	52.0 ± 1.8	53.6 ± 2.3
AuNP + PEG-trastuzumab (5 µg)	47.1 ± 1.3	52.1 ± 4.3	43.9 ± 3.0

^a This table depicts the stability of trastuzumab-PEG-AuNPs in 1% NaCl as a function of particle size (Z-average) when measured by DLS for 14 days at 4°C. Values represent the mean diameter (nm) ± SD from three independent experiments.

ratio was increased. There are 13 and 32 lysine residues per light and heavy chain respectively and a total of 90 lysine residues on trastuzumab that may be modified. The variable light chain of trastuzumab has 4 lysine residues (Lys 39, 42, 45 and 103). Modification of these lysine residues could decrease affinity for HER-2; however, our group³⁰ previously showed that modification of lysines on trastuzumab Fab with

diethylenetriaminepentaacetic acid (DTPA) for labeling with ¹¹¹In did not significantly diminish HER-2-binding affinity compared with nonderivatized Fab ($K_d = 47$ vs 36 nM; $P > .05$). None of the 25 lysine residues present in trastuzumab Fab was identified as essential for interaction with HER-2/neu by alanine scanning.³¹ Thus, we speculate that diminished receptor-binding affinity of PEGylated trastuzumab may be caused by steric hindrance as a result of PEG substitution on trastuzumab, an effect which is increased at higher ratios of OPSS-PEG-SVA:trastuzumab.

Thiol-containing molecules can interact with metal ions and metal surfaces to form covalent bonds.³² Mono- or bifunctional PEG of varying molecular weights has been used extensively to stabilize AuNPs.^{18,21,33} Our results suggest that AuNPs were effectively stabilized in 1% NaCl by reaction with a 7,500 molar excess of PEG-SH (MW = 2 kDa). These PEG-stabilized AuNPs showed an average increase in particle size of about 6.5 nm as determined by dynamic light scattering (DLS). Liu et al.¹⁸ have reported that PEGylation of AuNPs with PEG-SH (MW = 1.5 kDa) similarly increased the hydrodynamic radius of the AuNPs by 5 nm.

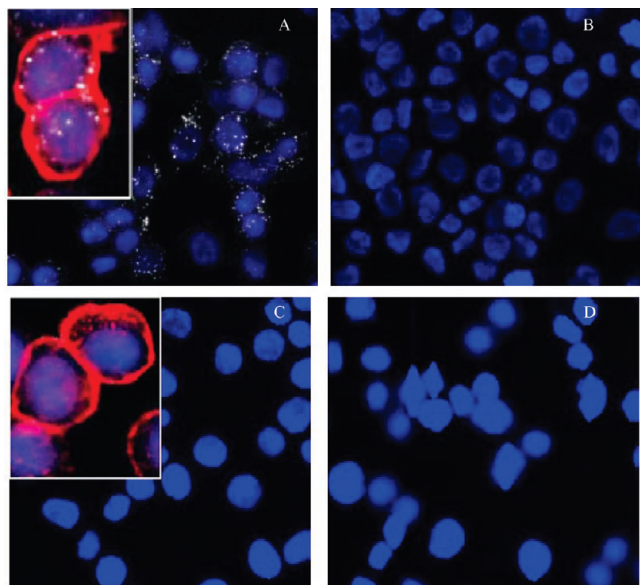


Figure 7. Darkfield microscopy of SK-BR-3 cells treated with (A, B) trastuzumab-PEG-AuNP or (C, D) PEG-AuNP. Panels B and D represent cells pretreated with 300 nM trastuzumab to block HER-2 receptors. The nucleus was visualized with DAPI (blue). Inset represents cells from a separate experiment stained with cell membrane marker wheat germ agglutinin-Alexa Fluor 594 (red). Light scattering due to internalization of AuNPs was detected only in SK-Br-3 cells treated with trastuzumab-PEG-AuNP (white, pseudocolor).

SDS-PAGE results suggested nonhomogenous substitution of PEG on trastuzumab at lower trastuzumab:PEG reaction ratios as evident from the laddering effect. At reaction molar ratios of OPSS-PEG-SVA:trastuzumab of 25:1 or greater, formation of PEGylated trastuzumab fractions with a narrower MW distribution was observed as evidenced by the presence of a single band. The band observed at 250 kDa or higher is most likely due to dimerized trastuzumab as a result of intermolecular cross-linking during the PEGylation reaction and has been previously observed with modification of amines on the antibody.³⁴ Size-exclusion HPLC further supports the hypothesis that, at lower molar reaction ratios, nonhomogenous PEGylation occurs noted as multiple peaks with t_R of 5.6 and 6.4 min when trastuzumab was reacted with OPSS-PEG-SVA at 1:1 and 10:1 ratios whereas a single peak with t_R of 5.6 min was found when trastuzumab was reacted with a 25-fold molar excess or higher molar ratios of OPSS-PEG-SVA. The quantitative measurement of antibodies conjugated to the surface of AuNPs is challenging.³⁵ AuNPs have strong light absorption through most of the visible and UV range and, consequently, provide high background when standard colorimetric protein determination methods are used. Eck et al.³⁶ found that even with the micro-bicinchoninic acid (BCA) assay, which has been widely used to quantify antibodies attached to AuNPs³⁵ and is one of the most sensitive colorimetric protein assays available,³⁷ the light absorption by the AuNPs themselves was an order of magnitude larger than that caused by assaying the conjugated proteins. Other researchers have used ELISA-based assays to

quantify the number of antibodies per AuNP.³⁸ Using the maximal adsorption density of ~ 2.5 mg IgG/m² of particle surface for IgG (or 100 nm²/IgG) reported by Cantarero et al.,³⁹ the number of intact IgG molecules that can form a monolayer on the surface of 30 nm diameter spherical nanoparticles has been calculated by Melancon et al.³⁵ as 28 per nanoparticle. Using a colorimetric assay, it was recently reported that 124 antibodies were attached to each 30 nm nanoparticle.³⁵ Lowery et al.³⁸ recently reported the conjugation of 152 ± 128 anti-HER-2 antibodies to gold nanoshells using an ELISA-based assay. The much higher surface modification with IgG than theoretically possible as well as the large variability in measurement suggests that these assays are not reliable for quantification of the number of antibodies conjugated to AuNPs. The use of ¹²⁵I-labeled PEG-trastuzumab as a radiotracer for accurately quantifying the number of antibodies conjugated to the surface of AuNPs by γ -scintillation counting thus represents a novel approach that circumvents the problems of protein measurements using colorimetric, fluorescence or immunological (i.e., ELISA) methods and yields values closer to the theoretical limitation for AuNP surface modification.

The data from TEM and DLS suggests that the trastuzumab conjugated to the AuNP via the longer length cross-linker (OPSS-PEG-SVA, MW = 5K) extends away from the AuNP surface beyond the PEG-SH (MW = 2 kDa) coating, thereby providing the greatest opportunity for unrestricted HER-2 binding. Therefore, using a combination of these short and long PEG chains, we were able to engineer a physically stable AuNP nanomaterial with HER-2 binding

- (30) Tang, Y.; Wang, J.; Scollard, D. A.; Mondal, H.; Holloway, C.; Kahn, H. J.; Reilly, R. M. Imaging of HER2/neu-positive BT-474 human breast cancer xenografts in athymic mice using ¹¹¹In-trastuzumab (Herceptin) Fab fragments. *Nucl. Med. Biol.* **2005**, *32*, 51–58.
- (31) Kelley, R. F.; O'Connell, M. P. Thermodynamic analysis of an antibody functional epitope. *Biochemistry (N.Y.)* **1993**, *32*, 6828–6835.
- (32) Hermanson, G. *Bioconjugate Techniques*; Elsevier: Netherlands, 2008; pp 1323.
- (33) Bhattacharya, R.; Patra, C. R.; Earl, A.; Wang, S.; Katarya, A.; Lu, L.; Kizhakkedathu, J. N.; Yaszemski, M. J.; Greipp, P. R.; Mukhopadhyay, D.; Mukherjee, P. Attaching folic acid on gold nanoparticles using noncovalent interaction via different polyethylene glycol backbones and targeting of cancer cells. *Nanomed. Nanotechnol. Biol. Med.* **2007**, *3*, 224–238.
- (34) Costantini, D. L.; Chan, C.; Cai, Z.; Vallis, K. A.; Reilly, R. M. ¹¹¹In-labeled trastuzumab (Herceptin) modified with nuclear localization sequences (NLS): An auger electron-emitting radiotherapeutic agent for HER2/neu-amplified breast cancer. *J. Nucl. Med.* **2007**, *48*, 1357–1368.
- (35) Melancon, M. P.; Lu, W.; Yang, Z.; Zhang, R.; Cheng, Z.; Elliot, A. M.; Stafford, J.; Olson, T.; Zhang, J. Z.; Li, C. In vitro and in vivo targeting of hollow gold nanoshells directed at epidermal growth factor receptor for photothermal ablation therapy. *Mol. Cancer Ther.* **2008**, *7*, 1730–1739.
- (36) Eck, W.; Craig, G.; Sigdel, A.; Ritter, G.; Old, L. J.; Tang, L.; Brennan, M. F.; Allen, P. J.; Mason, M. D. PEGylated gold nanoparticles conjugated to monoclonal F19 antibodies as targeted labeling agents for human pancreatic carcinoma tissue. *ACS Nano* **2008**, *2*, 2263–2272.

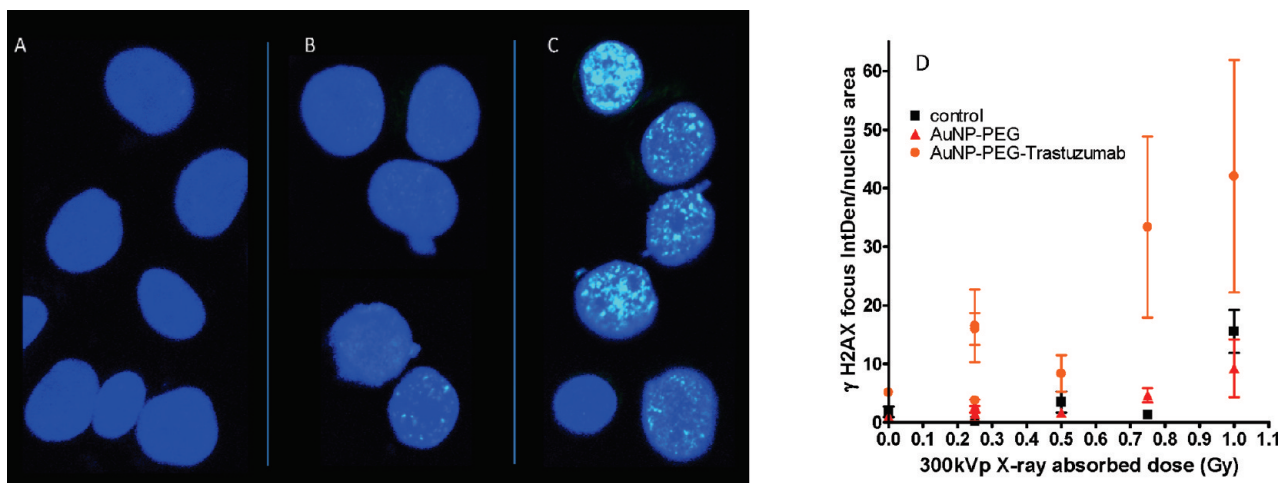


Figure 8. DNA double-strand break (DSB) induction in SKBR3 cells 30 min after being exposed to 0.25 Gy of 300 kVp X-rays in (A) cells treated with PBS, (B) cells treated with 0.3 nM (2×10^{11} particles/mL) of PEG-AuNP or (C) 0.3 nM (2×10^{11} particles/mL) trastuzumab-PEG-AuNP were determined by the γ -H2AX assay and imaging of the foci (green signal representing DNA DSB) using confocal microscopy. (D) The DNA double-strand break (DSB) induction as determined by the γ -H2AX assay was quantified as focus integrated density (InD) per unit nucleus area using ImageJ software. Data represent the mean \pm SD result from three independent experiments.

capability. Stability was imparted by modification of the AuNPs with the shorter PEG-SH (MW = 2 kDa) chains. Conjugation of trastuzumab to AuNPs using the longer OPSS-PEG-SVA linker (MW = 5 kDa) offers several advantages over direct physical adsorption of trastuzumab protein onto the nanoparticle surface: (1) known chemistry and more predictable orientation of trastuzumab to the AuNPs via the covalent bond between gold and the thiol on the PEG linker rather than random distribution as expected for physical adsorption,⁴⁰ (2) insertion of a flexible linker between the trastuzumab molecule and AuNPs that could allow trastuzumab to more effectively align with HER-2 for optimal binding and (3) by using an extended longer chain linker OPSS-PEG-SVA (MW = 5 kDa) to attach to AuNPs we hope to minimize any steric hindrance offered by the PEG-SH (MW = 2 kDa) used to stabilize the AuNPs.

The cellular uptake of nanoparticles is significantly influenced by their size and shape. Chithrani et al.¹⁶ have investigated the uptake of 14, 50, and 74 nm citrate-coated AuNPs in HeLa cells. It was found that the most efficient uptake occurred with 50 nm sized particles. The size of the trastuzumab-modified AuNPs in our study was similar to this

optimal dimension (i.e., 54–62 nm). TEM results with immunogold labeling provided visual evidence that multiple antibody molecules were attached to each 30 nm AuNP, which, combined with the PEGylation, increased the size to 54–62 nm. The presence of several trastuzumab-PEG molecules per AuNP could potentially enhance the avidity of interaction with HER-2 on breast cancer cells.⁴¹

Darkfield microscopy images (Figure 7) indicated that AuNPs, when conjugated to trastuzumab, were specifically bound and taken up by SK-BR-3 cells likely due to a HER-2 mediated endocytotic process, since little or no uptake was observed for AuNPs not conjugated to trastuzumab. Furthermore, the uptake of trastuzumab-PEG-AuNP was inhibited by preblocking HER-2 with an excess (300 nM) of trastuzumab. PEG modification generally reduces nanoparticle nonspecific cellular internalization which may be mediated, particularly *in vivo*, by adsorption of serum proteins onto their surface⁴² that induce endocytosis.⁴³ Some studies suggest that trastuzumab can promote internalization of HER-2.⁴⁴ This mechanism could facilitate internalization of trastuzumab-PEG-AuNPs. The internalized AuNPs were

- (37) Grabar, K. C.; Griffith Freeman, R.; Hommer, M. B.; Natan, M. J. Preparation and characterization of Au colloid monolayers. *Anal. Chem.* **1995**, *67*, 735–743.
- (38) Lowery, A. R.; Gobin, A. M.; Day, E. S.; Halas, N. J.; West, J. L. Immunonanosensors for targeted photothermal ablation of tumor cells. *Int. J. Nanomed.* **2006**, *1*, 149–154.
- (39) Cantarero, L. A.; Butler, J. E.; Osborne, J. W. The adsorptive characteristics of proteins for polystyrene and their significance in solid-phase immunoassays. *Anal. Biochem.* **1980**, *105*, 375–382.
- (40) Liu, Y.; Liu, Y.; Mernaugh, R. L.; Zeng, X. Single chain fragment variable recombinant antibody functionalized gold nanoparticles for a highly sensitive colorimetric immunoassay. *Biosens. Bioelectron.* **2009**, *24*, 2853–2857.

- (41) Hong, S.; Leroueil, P. R.; Majoros, I. J.; Orr, B. G.; Baker, J. R., Jr.; Banaszak Holl, M. M. The binding avidity of a nanoparticle-based multivalent targeted drug delivery platform. *Chem. Biol.* **2007**, *14*, 107–115.
- (42) Ehrenberg, M. S.; Friedman, A. E.; Finkelstein, J. N.; Oberdörster, G.; McGrath, J. L. The influence of protein adsorption on nanoparticle association with cultured endothelial cells. *Biomaterials* **2009**, *30*, 603–610.
- (43) Göppert, T. M.; Müller, R. H. Polysorbate-stabilized solid lipid nanoparticles as colloidal carriers for intravenous targeting of drugs to the brain: Comparison of plasma protein adsorption patterns. *J. Drug Targeting* **2005**, *13*, 179–187.
- (44) Rubin, I.; Yarden, Y. The basic biology of HER2. *Ann. Oncol.* **2001**, *12*, S3–S8.

not toxic to SK-BR-3 cells as determined in clonogenic assays (mean surviving fraction, 1.00 ± 0.22).

Hainfeld et al.⁴⁵ demonstrated remarkable effectiveness of 1.9 nm AuNPs administered iv in controlling the growth of EMT-6 murine mammary carcinoma tumors when used in conjunction with a local 30 Gy radiation dose delivered by 250 kVp X-rays. One-year survival was 86% versus 20% with X-rays alone and 0% with gold alone.⁵ Since these were nontargeted AuNPs the tumor accumulation could be attributed to the leaky vasculature of EMT-6 tumors.⁴⁶ In contrast, Jain et al.⁴⁷ studied 1.9 nm particles in conjunction with 160 kVp X-rays. They reported only a modest dose enhancement of 1.4 *in vitro* using MDA-MB-231 breast cancer cells in a clonogenic assay. In contrast, Rahman et al.⁴⁸ achieved a dose enhancement factor of 24.6 as assessed by a cell survival assay when bovine aortic endothelial cells were treated *in vitro* with 1 mM AuNPs (1.9 nm) in combined with 80 keV X-rays. These varied results pose several key questions including if it is essential to achieve intracellular delivery of AuNPs to achieve dose enhancement. Targeted AuNPs will accumulate initially in tumors due to their leaky vasculature as a consequence of the well documented enhanced permeation and retention (EPR) effect.⁴⁹ The presence of a targeting ligand on the surface of the AuNPs will then allow receptor mediated internalization into tumor cells. In a first attempt to study the radiosensitization effects of targeted AuNPs, Kong et al.⁵⁰ studied thioglucose modified AuNPs (Glu-AuNP) or cysteamine-modified AuNPs (AET-AuNP) in MCF-7 breast cancer cell lines in combination with 200 kVp X-rays. Their TEM results indicated that AET-AuNPs were mostly bound to the cell membrane, while Glu-GNPs entered the cells and were distributed in the cytoplasm. Interestingly, Glu-AuNPs had a lower fraction of cell survival than AET-AuNPs,

suggesting that internalization is necessary for AuNP mediated radiation dose enhancement. In the present study using the γ H2AX assay we observed that the induction of DSBs in trastuzumab-PEG-AuNPs treated cells was 5.1- and 3.3-fold higher than those in AuNP-PEG-treated cells and control cells. The modification of the AuNPs with trastuzumab allowed their specific binding to HER-2-overexpressing cells and exploited the receptor-mediated internalization process to deposit the AuNPs into the cytoplasm where collectively the Auger and photoelectrons enhanced the DNA damage following X-radiation of the cells.

Conclusion

We conclude that trastuzumab was successfully conjugated to 30 nm AuNPs, resulting in an increase in hydrodynamic size from 35 to 58 nm, but with good retention of immunoreactivity for HER-2. This targeted nanotechnology-based radiosensitizer was further characterized for its physicochemical properties and its specific binding and internalization into SK-BR-3 breast cancer cells *in vitro*. Experiments evaluating the extent of DNA double-strand breaks in these cells incorporating the targeted and nontargeted AuNPs and exposed to 300 kVp X-radiation suggested that HER-2 mediated internalization of AuNPs was essential to enhance DNA double-strand breaks. The internalized AuNPs without X-radiation were nontoxic to the cells as assessed by clonogenic assay. Studies are in progress to examine the effects of this enhancement in DNA damage on clonogenic survival. The design and approaches taken to surface modify and characterize trastuzumab-AuNPs described in this study would have application to other molecularly targeted AuNPs for cancer treatment.

Acknowledgment. This research was supported by a grant from the Canadian Breast Cancer Research Alliance (Grant 019374) to J.-P.P. and R.M.R. N.C. is supported by a Vanier Canada Graduate Scholarship from the Canadian Institute of Health Research, a predoctoral fellowship from the U.S. Army Department of Defense Breast Cancer Research Program (W81XWH-08-1-0519, P00002), and a predoctoral fellowship from the Connaught Fund, University of Toronto. The authors thank Dr. H. Heerklotz for use of a Zetasizer ZS for AuNP characterization. The authors acknowledge the contributions of Drs. J. Leyton, B. Calvieri and S. Doyle in flow cytometry and transmission electron microscopy experiments. The authors thank Ms. D. Scollard for reviewing the manuscript. Parts of this manuscript were presented at the European Association of Nuclear Medicine in Barcelona, Spain, October 10–14, 2009.

MP100207T

- (45) Hainfeld, J. F.; Slatkin, D. N.; Focella, T. M.; Smilowitz, H. M. Gold nanoparticles: A new X-ray contrast agent. *Br. J. Radiol.* **2006**, 79, 248–253.
- (46) Roberts, W. G.; Hasan, T. Tumor-secreted vascular permeability factor/vascular endothelial growth factor influences photosensitizer uptake. *Cancer Res.* **1993**, 53, 153–157.
- (47) In *2010 Genitourinary Cancers Symposium [Conference Proceedings]*; March 5–7, 2010; San Francisco, CA, USA; American Society of Clinical Oncology; 2010; p 126.
- (48) Rahman, W. N.; Bishara, N.; Ackerly, T.; He, C. F.; Jackson, P.; Wong, C.; Davidson, R.; Geso, M. Enhancement of radiation effects by gold nanoparticles for superficial radiation therapy. *Nanomed.: Nanotechnol., Biol., Med.* **2009**, 5, 136–142.
- (49) Peer, D.; Karp, J. M.; Hong, S.; Farokhzad, O. C.; Margalit, R.; Langer, R. Nanocarriers as an emerging platform for cancer therapy. *Nat. Nanotechnol.* **2007**, 2, 751–760.
- (50) Kong, T.; Zeng, J.; Wang, X.; Yang, X.; Yang, J.; McQuarrie, S.; McEwan, A.; Roa, W.; Chen, J.; Xing, J. Z. Enhancement of radiation cytotoxicity in breast-cancer cells by localized attachment of gold nanoparticles. *Small* **2008**, 4, 1537–1543.